STM JOURNALS

Journal of
Polymer & Composites

ISSN: 2321-2810 (Online)
ISSN: 2321-8525 (Print)
Volume 11, Special Issue 12, 2023
DOI (Journal): 10.37591/JoPC

http://engineeringjournals.stmjournals.in/index.php/JoPC/index

Research JoPC

Experimental Investigation of Thermally Grown Indium Film's Structural and Tribological Properties

Shailendra Kumar Gaur[1,2,*], Qasim Murtaza[3], R.S. Mishra[4]

Abstract

Indium thin film growth found numerous applications, such as cold welding of infrared detectors and readout-integrated circuits (ROIC) to form sensor chips. In film is grown on the Si substrate by thermal evaporation. The XRD results indicated the tetragonal bcc phase in the (101) preferential plane. Scanning electron microscopy (SEM) indicated an uniform, continuous film covering the whole surface. The EDS examination confirmed the pure In film. The atomic force microscopy (AFM) determined the average roughness and root mean square values at 38.5 nm and 47.9 nm, respectively. The ellipsometry measurement was done to check the surface condition and measure film thickness. The atomic force microscopy in contact mode determined the adhesion force 51.32 nN, thermodynamic adhesion-work according to the DMT and JKR theories 0.817 J/m^2 (DMT), 1.089 J/m^2, (JKR) and coefficient of friction 0.0049. The good adhesion of the film was tested via scotch tape.

Keywords: Thin film, indium, AFM, SEM, Adhesion force

INTRODUCTION

Indium is used as an interconnection in the microelectronics industry because it is a soft metal with a low melting point temperature. It is malleable and has a low coefficient of thermal expansion. Thermal evaporation synthesized nanoscale indium oxide films from pure indium on glass and quartz. The deposited films were annealed at 150-700°C for two to four hours and studied for their crystalline structure, morphological, optical, and electrical parameters. The annealing of the films improved the quality of the film and growth in one particular direction. The transmittance obtained was 83 %, and a band gap of 3.7 eV near bulk was received [1]. The process of RF sputtering was employed to deposit the indium films, and the deposited film was synthesized by changing the plasma control, oxygen pace, and procedure point in time durations. The film's structural, morphological, and electrical properties were analyzed, and it was found that the film was uniform, had good adhesion, and was void-free. Good electrical conductivity and particle sizes of 75-105 nm with low-roughness films were obtained [2]. Thin films of 100, 260, and 330 nm thicknesses were deposited on the glass substrate and examined using X-ray and transmission electron microscopy. At 100 nm, the film's cubic and tetragonal phases were present in In_2O_3 [3]. The SnO_2 thin-based gas sensor's performance was enhanced by doping. The intense change was observed at 20 wt. % of In by using $InCl_3$; however, the performance was drastically lowered above this wt% of In [4]. Nanoparticles were having good oil solubility and were used as a good lubrication agent. They showed good lubrication or antiwear properties of paraffin oil at low concentrations. If the nanoparticles' attention increased further, it significantly improved the efficiency of the lubricating agent [5]. In_2O_3 at the nanoscale in cubic phase was prepared by the hydrothermal flow synthesis reactor at elevated or

***Author for Correspondence**
Shailendra Kumar Gaur

[1] Research Scholar, Department of Mechanical Engineering, Delhi Technological University, Bawana road, Delhi, India,
[2]Technical Officer C, Solid State Physics Laboratory, Timarpur, Delhi, India
[3] Professor, Department of Mechanical Engineering, Delhi Technological University, Bawana road, Delhi, India,
[4] Professor, Department of Mechanical Engineering, Delhi Technological University, Bawana road, Delhi, India,

Received Date: October 30, 2023
Accepted Date: November 20, 2023
Published Date: February 28, 2024

Citation: Shailendra Kumar Gaur, Qasim Murtaza, R.S. Mishra. Experimental Investigation of Thermally Grown Indium Film's Structural and Tribological Properties. Journal of Polymer & Composites. 2023; 11(Special Issue 12): S58–S66.

higher temperatures such that no indium hydroxide was formed. The prepared In_2O_3 in powder form was used in sensor applications. The gas sensor substrate was an Au electrode on an Al_2O_3 tile, and the indium oxide sensor was made by a drop coating of 2 or 3 12 µL droplets of water-based paste of nanoscale particles [6]. A thin film of thickness 10–40 nm was deposited by the vacuum evaporation method on the CdZnS, which was deposited by a chemical reaction between cadmium acetate, thiourea, ammonia, and ammonium acetate on a glass substrate. The formation of the In_2O_3 layer acted as an insulator, prevented the oxidation of CdZnS, and allowed the diffusion of In into it. Thus, it enhanced the conductivity of the CdZnS film and prevented oxidation, which could be utilized in solar cell applications [7]. The film was deposited by the thermal evaporation method on Si (100) of p-type and further annealed. The In_2O_3 layer was prepared devoid of using any catalyst, and it was a self-assembled mechanism using In film annealed in a tube furnace. Thus, nanowires and nanorods developed on the Si surface [8]. Si nanowires were developed on a coated Si substrate by the electron beam evaporation method using Si ingot. In was on top of each Si nanowire, indicating the VLS growth, and EDS analysis confirmed the presence of the In nanoparticle [9]. Indium tungstate was deposited from WCl_6, $InCl_3$, and CH_3CN in a glass ampoule located in a glove box as well as heated by 130°C for seven days. The resultant mixture heated first at 400°C and then up to 700°C for 3 hours to obtain the crystalline structure. The XRD examination revealed that it was unsuitable for a regulated thermal expansion composite and exhibited a pressure-induced phase transition [10].

Present investigation deals with Indium (In) film grown on Si substrate by the thermal evaporation method and the deposited film for structural, morphological, topographical, and tribological properties. The film was checked for the suitability of indium bump growth used in an infrared detector and readout integrated circuit (ROIC).

MATERIALS AND METHODS

The thermal evaporation method was used to grow In film on Si substrate. The base vacuum in the chamber was 1 x 10^{-6} mbar, and the section was cleaned thoroughly before deposition. After cleaning, the room was evacuated to 1 x 10^{-6} mbar, and the empty molybdenum boat was heated. The indium small shots of purity 99.999 % were placed in the ship. The quartz crystal set close to the Si substrate monitored the deposition rate and thickness. The boat was heated resistively to melt the In small shots, and the source shutter was removed after 5-7 s. The crystallographic structure was measured using an XRD unit from PAN analytical B.V. Xpert PRO with a CuKα (wavelength, = 1.542Å). The morphologies, microstructures, and compositional were analyzed by Field Emission Electron Microscopy (FESEM) Model - FESEM Carl Zeiss SUPRA55VP and Oxford instrument X-MAX EDS spectrometer. The film's surface roughness and adhesion characteristics were analyzed using the atomic force microscopy Model - 5600 LS AC III module of Agilent technologies. The tribological properties were measured by AFM in contact mode using force microscopy. An Ellipsometry of In film was done using the LSE-MS STOKES Ellipsometer Model 7109-C370M from GAERTNER. The He-Ne laser was used, measuring at an angle of 70°, and the wavelength used $\boldsymbol{\lambda}$ = 6328 Å. The adhesion of the film on the Si surface was tested by scotch tape.

Figure 1 showed the Schematic diagram of 6 µm indium film grown on the 650 µm thick Si substrate. The white shiny surface appeared on the Si surface after deposition over the entire Si surface.

RESULTS & DISCUSSION

X-ray Diffraction Investigation

The XRD diffractogram of the In was shown in Figure 2. The intense XRD peak was related to the tetragonal bcc phase corresponds to (101) preferential plane at about 2θ = 33.05°. The other XRD peaks obtained at 36.46°, 39.25°,54.49°, 63.29°, and 67.11° related to (002), (110), (112), (103) and (211) planes, respectively. The XRD peak obtained at 2θ = 56.68° corresponds to the Si substrate. The good, sharp narrow peaks indicated the good crystallinity of the indium film. The XRD results

obtained were very well matched with the earlier reported results [11, 12]. The crystallite size (D) of the indium film was determined using Debye-Sherrer eq. (1) [13] [16]

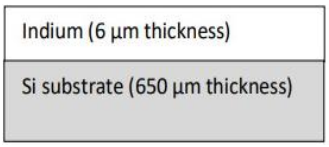

Figure 1. Schematic diagram of indium film on Si substrate.

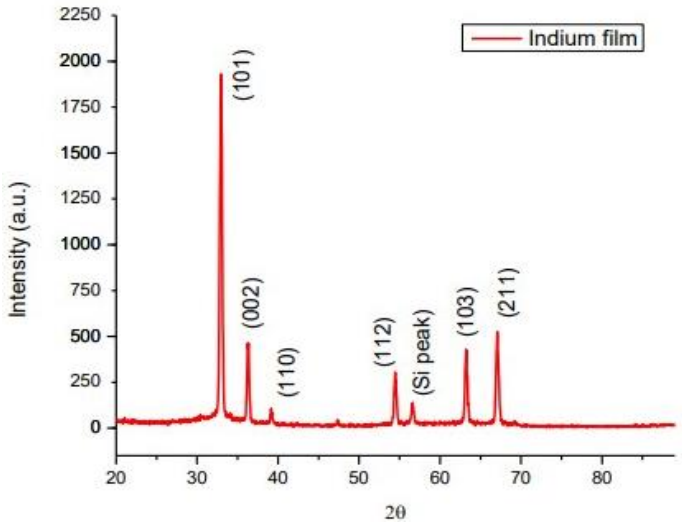

Figure 2. XRD pattern of indium film.

$$D = 0.94\lambda/\beta Cos\theta \quad (1)$$

where β was the full width half maximum, θ was the angle of diffraction and **λ** (1.54) was the wavelength of the X-ray used. The dislocation density(δ) as well as strain(ε) of the film was determined using the eq.(2) and (3) [13,14] Indium (6 µm thickness) Si substrate (650 µm thickness).

$$\delta = 1/D^2 \quad (2)$$

$$\varepsilon = \beta/4Tan\theta \quad (3)$$

The number of crystallites per unit area of the film was determined using the eq. (4) [15].

$$N = t/D^3 \quad (4)$$

where t was the film thickness. The crystal structure parameters of the In film on Si substrate were shown in Table 1. According to the Table 1, we found 24.2 nm was the crystallite size for the dominant XRD peak at (101) plane

Morphology and Composition Analysis

The SEM micrographs of the surfaces of the grown indium film by the thermal evaporation process were revealed in Figures. 3 (a) and 3(b). The SEM micrographs show that the film was pinhole-free, uniform, and continuous over the entire Si surface. However, a few about 1-3 µm-sized particles were lying on the surface, but there were no cracks or other discontinuities in the film.

The compositional analysis of In film was done by energy dispersive spectroscopy (EDS) to determine the purity of the In film. The EDS images were indicated by Figures 4 (a) and (b). Figure 4(a) showed the EDS image at 1.15 KX magnification, and Figures 4(b) showed the spectrum of the EDS examination. In Table 2, the overall elemental analysis of the indium film was given. From EDS analysis, we found that pure In was present at 52.61 % atomic percentage and 91.39% weight percentage. A small amount of C present in the film which may be due to contamination of film

during the growth. Thus, the EDS analysis of In film was comparable with the previously reported examination of In deposited by electrochemical deposition technique [16].

Table 1. Crystal structure parameters of indium film.

hkl	θ (°)	β (°)	D (nm)	δ (x 10^{11}) (lines/cm^2)	ε (x 10^{-3})	N (x 10^{13}) (cm^{-2})
(101)	16.52	0.357	24.2	1.70	5.24	4.21

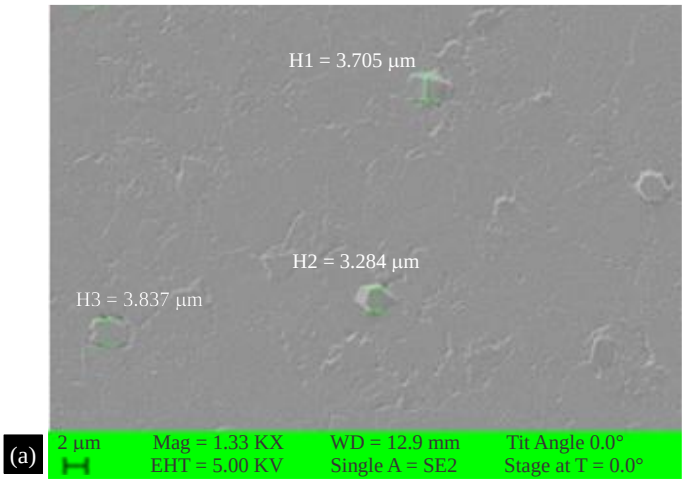

(a)

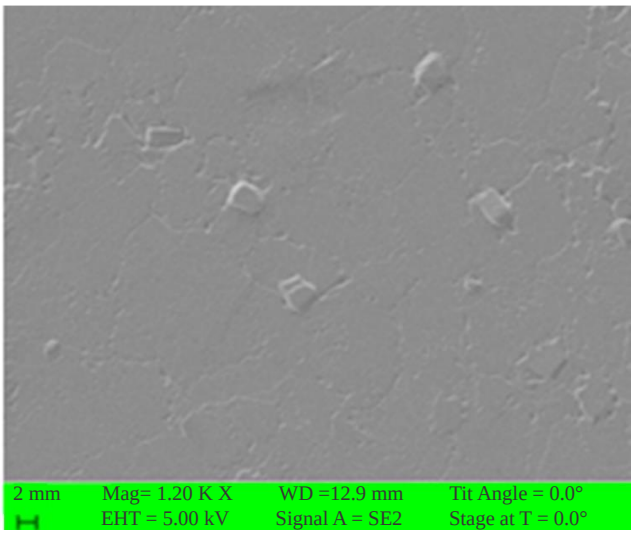

(b)

Figure 3. In film SEM plan view (a) image at 1.36 KX magnification (b) image at 1.39 KX magnification

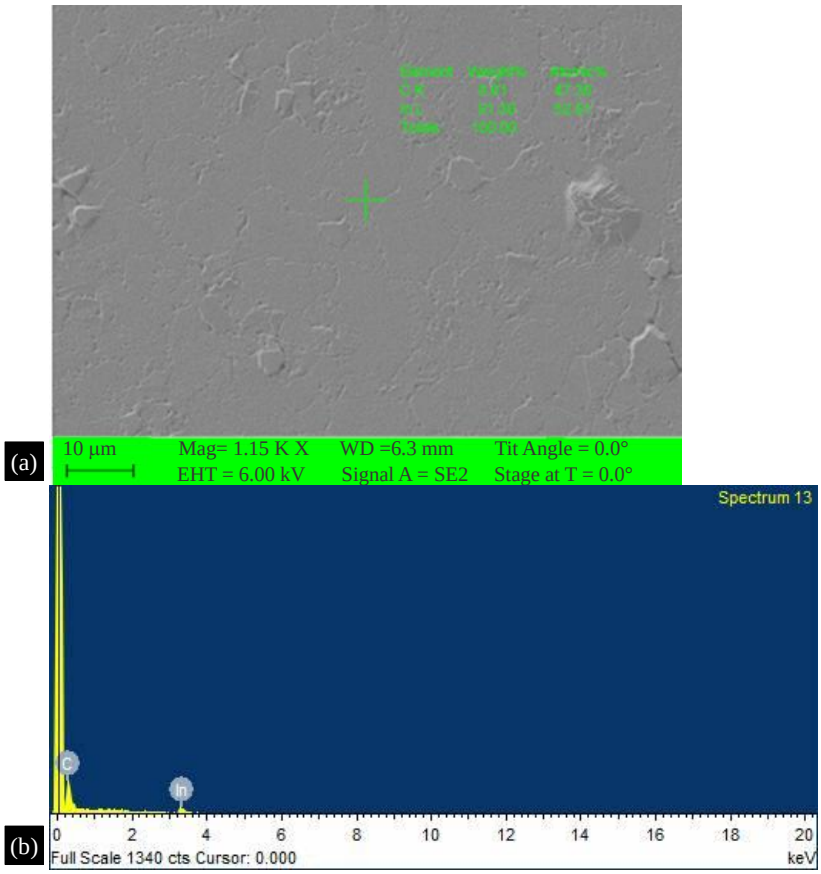

Figure 4. Indium film (a) EDS image at 1.15 magnification (b) EDS spectrum graph.

Table 2. EDS compositional analysis of Indium films

Thickness (µm)	Atomic%		Weight %	
	In	C	In	C
6	52.61	47.39	91.39	8.61

Surface Topography Analysis

The AFM-scanned two-dimensional and three-dimensional images of the In film were indicated by Figures 5(a) and 5(b), respectively. Based on AFM examination, we found that the film had rough but uniform coverage. The In film's average and rms roughness values were 38.5 nm and 47.9 nm, respectively. The In film's roughness values were shown in Table 3.

The Rz was the difference between the tallest peak and the deepest valley on the surface. The roughness skewness (Rsk) was the roughness value of the film, which was related to the departure of the surface from symmetry. The roughness kurtosis (Rku) was the roughness value of the film related to the sharpness of the roughness profile.

Ellipsometry Analysis

The ellipsometry anlysis is identified by two parameters, psi (ψ) and delta (Δ). It measures the complex reflection ratio.

$$\rho = r_p/r_s = \text{Tan } \psi . e^{i\theta} \quad (5)$$

where r_p and r_s are Fresnel reflection coefficients. Tan ψ is the amplitude ratio after reflection, and Δ is the phase difference. The ellipsometry measurement of in film was done to determine the quality of the surface and the film thickness by using eq. (5). In film's ellipsometry parameters psi (ψ), delta

(Δ), and film thickness were measured at three different points, which are shown in Table 4. The three measurement points are taken such that one was at the center of sample and two were diagonally opposite each other. From Table 4, we observed that the film thickness value indicated by the quartz crystal was nearly the same. The ψ and Δ values of the film were consistent at all three measurement points and comparable to the previously reported values [17].

Determination of Adhesion Force and Friction Force

The force consequential from the molecular contact between two solids in contact determines adhesion at the contact interfaces. Based on Johnson, Kendall, and Roberts (JKR) and Derjaguin, Muller, and Toporov (DMT), a minimum load can be called the pull-off force or adhesion force. The AFM force spectroscopy gives a force distance curve (f-d curve) to realize the tip-film interactions and mechanical characteristics at a particular region of the film. This is often also called AFM dynamic mode scanning. The In film's AFM force-distance curve was shown in Figure 6, which indicated the tip trace and retrace profiles over the surface. The thermodynamic adhesion-work is explained by the DMT and JKR theories:

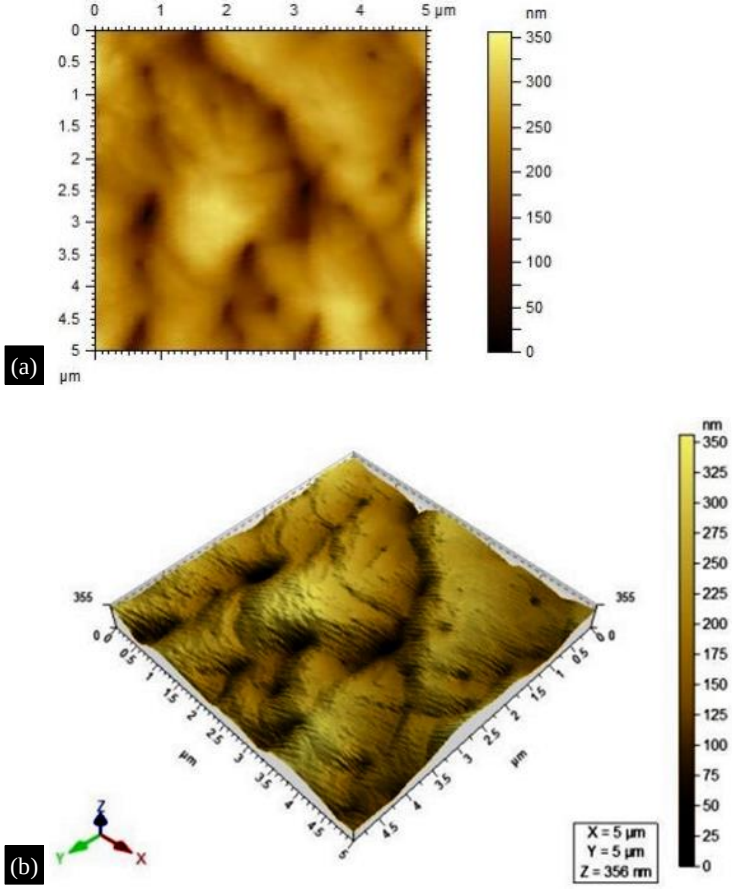

Figure 5. AFM images of In film (a) 2-dimensional image (b) 3-dimensional image.

Table 3. Roughness values of indium film

Thickness (μm)	R_a (nm)	R_q (nm)	R_z (nm)	R_{sk}	R_{ku}
6	38.5	47.9	356	0.261	2.99

Table 4. Ellipsometry parameters ψ, Δ, and film thickness of indium film

Film thickness (μm)	Measurement at position 1			Measurement at position 2			Measurement at position 3		
	Ψ (°)	Δ(°)	Thickness	Ψ(°)	Δ(°)	Thickness	Ψ(°)	Δ(°)	Thickness

			(μm)			(μm)			(μm)
6	40.52	123.16	5.95	40.48	123.52	5.96	40.08	124.13	6.03

$$FDMT = -2\pi\omega R \quad (6)$$

$$FJKR = (-3/2)\,\pi\omega R \quad (7)$$

Both friction force and pull-off force were measured at a scan size of 5 μm × 5 μm at a load of 50 nN. The AFM probe used a force constant of 0.0030-0.13 N/m and a radius less than 15 nm.

The frictional force, based on torsion beam theory, between the AFM probe and in films can be calculated using eq. (8):

$$F_f = (dzrGh^3b)/(l^2s) \quad (8)$$

where dz was the friction signal, G was the AFM tip shear modulus, r was a constant (r = 0.33), and b,s,l,h were the geometrical parameters of the tip in μm. The adhesion force, thermodynamic work of adhesion, friction signal, and coefficient of friction of In film were shown in Table 5. The adhesion force, thermodynamic work of adhesion (DMT &JKR) and coefficient of friction of In film were 51.32 nN, 0.817 J/m^2 (DMT) 1.089 J/m^2 (JKR) and 0.0049, respectively.

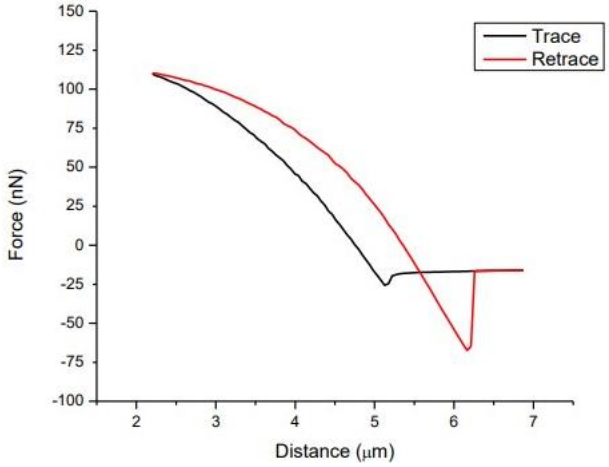

Figure 6. AFM force-distance(f-d) curve.

Table 5. Adhesion force, work of adhesion, friction signal, force of friction and friction-coefficient of indium film.

Film thickness (μm)	Adhesion force (nN)	Work of adhesion, ω_{JKR} (J/M^2)	Work of adhesion, ω_{DMT} (J/M^2)	d_z (V)	F_f (nN)	Coefficient of friction, μ
6	51.32	0.817	1.089	0.0127	0.246	0.0049

The obtained values of adhesion-force as well as thermodynamic adhesion-work of In film were less than the previously reported values of Au and other metal films, which may be due to differences in densities as In is a soft metal and different pattern of grains distributions [18 19].

Testing of In Film's Adhesion

The Scotch tape test of In film ascertained good adhesion as the film was not removed with scotch tape from the Si surface. The In film was compatible with the metal bump requirement for interconnection between infrared focal plane arrays and readout-integrated circuits (ROIC).

CONCLUSIONS

The structural and tribological properties of the thermally grown In film on Si substrate were investigated. The XRD revealed the polycrystalline tetragonal bcc phase. The SEM images showed that the film was free from cracks and pinholes. The film was dense and had uniform coverage over the entire surface. The EDS spectrum indicated the deposited film was pure In, and the weight % was 91.39. The AFM scanning showed a rough surface with rms roughness value of 47.9 nm. The ellipsometry-measured values Ψ and Δ of the indium film surface were about 40.0° and 123°, respectively. The adhesion force, thermodynamic work of adhesion, friction force, and coefficient of friction were determined from the experimental AFM f-d curve. The film's low friction force and coefficient of friction were observed. Thus, measuring observed structural and tribological properties in cinema is recommended as a reasonable bump requirement in the cold welding of infrared detectors and readout-integrated circuits (ROIC).

Acknowledgement

The author acknowledges the director SSPL for supporting and helping for this work. The author also acknowledges the CEO STARC for supporting this work.

REFERENCES

1. Parveen Jain , Sukhvir Singh , Avanish Kumar Srivastava , Sandeep Kumar Pundir, Azar Majid Siddiqui , "Relevance of microstructure on optical properties of thermally evaporated indium oxide thin films " , Open Access Library Journal , 2 (2015) e 1200
2. S. Shanmugan, D. Mutharasu , "Surface and electrical properties of rhombohedral In2O3 thin films prepared by an O2 plasma process" , Journal of Ceramic Processing Research , 12 ,5 (2011) 57 8–582
3. K. Ulutas, D. Deger, N. Kalkan , S. Yildirim, Y. G. Selebi , Y. Iskarlatos , M. L. Ovecoglu , A. Genc , " Structural properties of In-In2O3 composite films " , IOP Conf. Series : Materials Science and Engineering 15 (2010) 012095
4. A. Salehi , M. Gholizade, "Gas-sensing properties of Indium-doped SnO2 thin films with variation in indium concentration" , Sensors and Actuators B , 89 (2003) 173–179
5. Yanbo Zhao, Zhijun Zang, Hongxin Dang, "A novel solution route for preparing indium nanoparticles " , Journal of Physical Chemistry B, 107 (2003) 7574–7576
6. Sofia Elouali, Leanne J. Bloor , Russell Binions , Ivan P. Parkin, Claire J. Carmalt, Jawwad A. Darr , " Gas sensing with nano-indium oxides (In2O3) prepared via continuous hydrothermal flow synthesis " , American Chemical Society, Langmuir , 28 (2012) 1879–1885
7. Jay-Hyeong Lee, Woo-Chang Song, Jun-Sin Yi , Yeong-Sik Yoo, " Characteristics of the CdZnS thin film doped by thermal diffusion of vacuum evaporated indium films", Solar Energy Materials & Solar Cells , 75 (2003) 227- 234
8. Mohsen Shariati , Vahid Ghafouri, "The annealing investigation on morphology and photoluminescence properties of In2O3 1-D nanostructures in resistive evaporation mechanism " The European Physical Journal Applied Physics , 65 (2014) 20404
9. R. Rakesh Kumar , K. Narasimha Rao , R. R. Phani, "Growth of Si nanowires by electron beam evaporation using In catalyst " , Materials Letters 66 , (2012) 110–112
10. Tamam I. Baiz, Christophe P. Heinrich , Nathan A. Banek , Boris L. Vivekens, Cora Lind, "In-situ non-ambient X-ray diffraction studies of indium tungstate", Journal of Solid State Chemistry, 187 (2012) 195- 199
11. Philip N. Bartlett, David Cook, C.H. (Kees) de groot, Andrew H. Hector, Ruomeng Huang, Andrews Jolleys, Gebriela P. Kissling, William Levason, Stuart J. Pearce , Gillian Reid, "Non-aqueous electrodeposition of p-block metals and metalliods from halometallate salts " , Journal of the royal society of chemistry , 3 (2013) 15645–15654
12. Zhiwei Li, Xiaojun Tao, Yaming Cheng, Zhishen Wu, Zhijun Zhang, Hongxin Dang, "A simple and rapid method for preparing indium nanoparticles from bulk indium via ultrasound irradiation", Materials Science and Engineering A , 407 (2005) 7–10
13. C. Aparna, Pramoda Kumara Shetty, M.G. Mahesha , I. Yashodhara, N. Karunakara, "Sensitivity estimation of indium oxide thin film for gamma sensing", Journal of Mat. Sci. , 58 (2023) 11374-

11391
14. P. Prabhukanthan, T. Rajesh Kumar, G. Harichandran, “Structural, morphological, optical and electrical properties of chemically deposited thin films of ZnSe”, International Journal of Innovative Research in Science and Technology,) vol. 2, issue 5 , (2014) ISSN (online) 2347–3207
15. G. Rakhymbay, M.K. Nauryzbayev, B.D. Burkitbayeva, A.M. Argimbaeva, R. Jumanova, A. P. Kurbatov , M. Eyraud, P. Kanuth, F. Vacandio, “Electrochemical deposition of Indium : Nucleation mode and diffusional limitation”, Russian Journal of Electrochemistry , vol. 52, no 2 (2016) 115- 122
16. J. Zang , Y. Zeng , D. Zhao , S. Yang , L. Yang , Z. Liu , R. Zang , W. Wang , D. Zang and L. Chen , “Ellipsometric study on size-dependent melting point of nanometer-sized indium particles” Physical Chemistry , 120 (2016) 10686- 10690.
17. Corina Birleanu, Marius Pustan, Violeta Merie, Raluca Muller, Rodica Voicu, Angela Baracu, S Cracium , “Temperature effect on the mechanical properties of gold nano films with different thickness” , IOP Conf. Series : Materials Science and Engineering 147 (2016) 012021
18. Corina Birleanu, Marius Pustan, Raluca Muller, Cristian Dudescu, Violeta Merie, Rodica Voicu, Angela Baracu, “Experimental investigation by atomic force microscopy on mechanical and tribological properties of thin films”, International Journal of Mater. Res. 107 (2016) 1–10

